UC Irvine
UC Irvine Previously Published Works

Title

South Pole Antarctica observations and modeling results: New insights on HOx radical and sulfur chemistry

Permalink

https://escholarship.org/uc/item/38n5415t

Journal

Atmospheric Environment, 44(4)

ISSN

1352-2310

Authors

Mauldin, Roy
Kosciuch, Edward
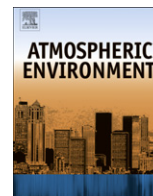Eisele, Fred
et al.

Publication Date

2010-02-01

DOI

10.1016/j.atmosenv.2009.07.058

Peer reviewed

South Pole Antarctica observations and modeling results: New insights on HOx radical and sulfur chemistry

Roy Mauldin [a],*, Edward Kosciuch [a], Fred Eisele [a], Greg Huey [b], David Tanner [b], Steve Sjostedt [b], Don Blake [c], Gao Chen [d], Jim Crawford [d], Douglas Davis [b]

[a] National Center for Atmospheric Research, Atmospheric Chemistry Division, 1850 Table Mesa, Boulder, CO 80305, USA.
[b] School of Earth and Atmospheric Sciences, Georgia Institute of Technology, Atlanta, GA 30332, USA
[c] University of California, Irvine, CA 92697, USA
[d] National Aeronautics and Space Administration, Langley Research Center, Hampton, VA 23681, USA

ARTICLE INFO

ABSTRACT

Measurements of OH, H_2SO_4, and MSA at South Pole (SP) Antarctica were recorded as a part of the 2003 Antarctic Chemistry Investigation (ANTCI 2003). The time period 22 November, 2003–2 January, 2004 provided a unique opportunity to observe atmospheric chemistry at SP under both natural conditions as well as those uniquely defined by a solar eclipse event. Results under natural solar conditions generally confirmed those reported previously in the year 2000. In both years the major chemical driver leading to large scale fluctuations in OH was shifts in the concentration levels of NO. Like in 2000, however, the 2003 observational data were systematically lower than model predictions. This can be interpreted as indicating that the model mechanism is still missing a significant HO_x sink reaction(s); or, alternatively, that the OH calibration source may have problems. Still a final possibility could involve the integrity of the OH sampling scheme which involved a fixed building site. As expected, during the peak in the solar eclipse both NO and OH showed large decreases in their respective concentrations. Interestingly, the observational OH profile could only be approximated by the model mechanism upon adding an additional HO_x radical source in the form of snow emissions of CH_2O and/or H_2O_2. This would lead one to think that either CH_2O and/or H_2O_2 snow emissions represent a significant HO_x radical source under summertime conditions at SP. Observations of H_2SO_4 and MSA revealed both species to be present at very low concentrations (e.g., 5×10^5 and 1×10^5 molec cm^{-3}, respectively), but similar to those reported in 2000. The first measurements of SO_2 at SP demonstrated a close coupling with the oxidation product H_2SO_4. The observed low concentrations of MSA appear to be counter to the most recent thinking by glacio-chemists who have suggested that the plateau's lower atmosphere should have elevated levels of MSA. We speculate here that the absence of MSA may reflect efficient atmospheric removal mechanisms for this species involving either dynamical and/or chemical processes.

© 2009 Elsevier Ltd. All rights reserved.

1. Introduction

The South Pole (SP) remains a unique environment in which to perform atmospheric studies focused on HO_x–NO_x chemistry. At first glance, the combination of low sun angle and low atmospheric water content would suggest very low oxidant levels, thus making it a region displaying minimal photochemistry. However, findings from earlier studies (Investigation of Sulfur Chemistry in the Antarctic Troposphere, ISCAT 1998, 2000) have shown this expectation to be out of date (Chen et al., 2001, 2004; Davis et al., 2001, 2004a,b,c, 2008; Mauldin et al., 2001a, 2004; Wang et al., 2008). In fact, the observational data have shown that the diurnal average OH concentration on the plateau is similar in magnitude to that found in the tropical-marine boundary layer (MBL) (Mauldin et al., 2001a, 2004). This finding is much related to the another surprise finding, namely, high levels of the trace gas nitric oxide (NO) are typically present (Davis et al., 2001, 2004a,b,c, 2008). Research at several different polar sites has now demonstrated that these elevated levels of NO are a result of releases of NO_x from the snow-pack due to the photolysis of nitrate (Honrath et al., 1999, 2000; Jones et al., 2001; Davis et al., 2001).

In sharp contrast to the OH observations, measurements of gas phase H_2SO_4 and MSA have shown very low concentrations for both

species (i.e., $<5 \times 10^5$ molec cm^{-3}) [Mauldin et al., 2001a, 2004]. Combined with aerosol sulfate and methane sulfonate observations (Arimoto et al., 2001, 2004), these low values suggest that local production of H_2SO_4 and MSA from marine biogenic species such as dimethyl sulfide (DMS) contributes very little to the atmospheric aerosol loading at SP.

In this work we present yet another SP OH, H_2SO_4, and MSA data set as well as the first measurements of SO_2. These new observations were recorded during the Antarctic Tropospheric Chemistry Investigation (ANTCI 2003) study. This expanded OH as well as NO data set has allowed for yet another detailed examination of the close coupling between HO_x and NO_x species under SP conditions. In addition, it has provided a first of its kind look at this complex chemical system during a solar eclipse event (i.e., 23 November, 2003). This new study has also provided a basis for more fully exploring the chemical and physical processes involved in the formation and loss of sulfur species, i.e., H_2SO_4 and MSA. In particular, we present arguments related to there being highly efficient MSA removal processes operating on the plateau.

2. Sampling site, instrumentation, and model description

2.1. Sampling site and instrumentation

The ANTCI 2003 study was conducted during the months of November and December and was based in the Atmospheric Research Observatory (ARO) at the Amundsen-Scott South Pole Station. OH measurements were made from the second floor of the observatory, placing the inlet at ∼10 m above the snow and extending ∼0.15 m beyond the building's outer wall. This wall was geographically oriented such that it faced into the prevailing winds. The observatory itself is located at the apex of the clean air sector, a 120° pie shaped sector at SP into which the prevailing wind blows. It is also a sector in which all human activity is greatly limited. Further details of the uniqueness of this sampling site can be found in Davis et al. (2001, 2004a).

The technique used for measuring OH, H_2SO_4, and MSA was selected-ion chemical-ionization mass spectrometry (SICIMS). This technique has been discussed in detail previously (e.g., Tanner et al., 1997; Mauldin et al., 1998, 1999 and references therein), and the reader is directed to those works for experimental details. These measurements were carried out in the same manner as described for the ISCAT 1998 and 2000 studies (e.g., Mauldin et al., 2001a, 2004).

As during ISCAT 2000, special measures were taken to assure that the H_2SO_4 and MSA measurements were free of particle evaporation effects. This was of considerable concern due to these species having enhanced vapor pressures upon entering the SICIMS sample inlet which typically is warmer than the outside air temperature. As in ISCAT 2000, this problem was minimized in the 2003 study by insulating the inlet. Periodic measurements were also made with a plastic straw denuder system as described in Mauldin et al. (2004). This device was designed to remove both OH and gas phase H_2SO_4, but allow the passage of particles. Results from these tests revealed 5 min average values for OH and H_2SO_4 of ∼4×10^4 molec cm^{-3}; thus demonstrating that particle evaporation had an insignificant impact upon observations of these species.

Calibrations were routinely carried out every 5–7 days with the results showing a variation of 19% (2σ). The average calibration coefficient over the duration of this study (e.g., the numerical value by which the ratio of sulfate to nitrate signal is multiplied by to obtain a concentration) was estimated at 3.07×10^9 molec cm^{-3}. This value compares quite well with that estimated during the ISCAT 2000 study (3.06×10^9 molec cm^{-3}). (The authors note that no ISCAT 1998 OH data have been included in this text for two reasons: 1) there remain unresolved OH calibration issues

associated with this older data set; and 2) no CH_2O or H_2O_2 measurements were recorded during the 1998 study, thus all model runs for this year lack this important HO_x source).

The uncertainty in the current set of measurements is estimated at ±40% for OH. H_2SO_4, and MSA. The cited error value is 2σ and was evaluated from a propagation of errors that included both the potential systematic and the estimated random errors for a given measurement. Even so, it must be acknowledged that there still is no quantitative way to estimate errors associated with possible sampling inlet losses. As briefly discussed in a study by Tanner and Eisele (1995), cross-winds can reduce the amount of OH, H_2SO_4, and MSA being measured by disturbing flows in the instrument's sampling tube. In the specific case of the ARO building, the sampling tube had to be lengthened to reach through the thick insolated building wall; thus, it was not possible to extend it much beyond the building's outside wall. And since the sampling tube itself could not be significantly lengthened without incurring substantial internal wall losses, most likely it rarely extended beyond the boundary layer air associated with the building's outer wall. Particularly for OH, building wall effects resulting from the release of chemicals or their serving as a chemical scavenging surface would in all likelihood further increase any potential wind induced losses at the entrance to the sampling tube. For sampled air approaching normal to the ARO wall, any building wall effect might be small except that the air stream might significantly decelerate and become nearly stagnant at the building surface. In this case it is likely that it would slowly flow parallel to the surface past the sample inlet. For air approaching nearly parallel to the building wall, a boundary layer would most likely form which would increase in depth as the air travelled along the wall. However, since the ARO outer wall has bubble windows that extend out beyond the OH sample tube inlet these windows might actually lead to a further increase in the thickness of the building's turbulent boundary layer.

Viewed more optimistically, the ARO building is well sealed with a metal outer skin which typically has an outside temperature of −25 to −40 °C. Thus, building emissions should be minimal. Winds are rarely calm, so airflow past the building is huge and nearly all sampling during the field study involved winds having a major vector component pointing toward the wall where sampling occurred. This suggests that sampled air probably found its way into the inlet before it ever reached the wall.

Different wind directions typically correspond to different air trajectories from the plateau, and hence, can involve quite different chemical histories. For this reason wind direction effects are difficult to study. Also, because the sample inlet was about 10 m above the snow surface there was no simple way that controlled tests could be carried out to test for any of the above effects. While no estimates of building induced losses can be given here, it should be noted that it is very unlikely that any of the three measured compounds were enhanced in concentration by the building, but it is quite possible that their concentrations were reduced.

2.2. Model description

Model simulations of OH were performed using a time-dependent photochemical box model developed at Georgia Tech and NASA Langley Research Center. A discussion of HO_x results from this model from the 2000 ISCAT study at SP can be found in Chen et al. (2004). A more detailed description of the kinetic/photochemical processes in this model has been given by Crawford et al. (1999) and Olson et al. (2003), thus only a brief description will be given here. The time-dependent box model contains 48 explicit reactions for HO_x–NO_x–CH_4 chemistry and >120 reactions to parameterize NMHC chemistry. The latter chemistry represents a modified form of the condensed mechanism of Lurmann et al. (1986). Typical inputs include temperature, pressure, NO, CO, O_3, and H_2O.

However, the model can also be constrained based on measured concentrations for the species OH, HNO_3, CH_2O, H_2O_2, HONO, or, HO_2NO_2. (Note, in the current paper, with the exception of the solar eclipse event, only observational data points for which measured values of CH_2O and H_2O_2 were reported have model results been cited.) J values for O_3 and NO_2 were derived from spectral actinic flux measurements recorded by Biospherical Instrument Inc. All other J values were scaled to these two based on TUV calculations (code available at http://cprm.acd.ucar.edu/Models/TUV). Since under typical SP summertime conditions no diurnal solar shift occurs, photochemical steady-state conditions were assumed in all model calculations. This same approximation was also applied on 23 November at the time of the solar eclipse. Quite noteworthy also is that variations in the model's J values were adjusted for the effects from shifts in the overhead O_3 column density as well as from local cloud coverage. Values for the former were obtained from NOAA's Boulder Research Lab.

First order loss rates for heterogeneous removal processes involving soluble species were taken from Slusher et al. (2002). The uncertainty estimated for the reported model runs is 35% and is based on Monte Carlo simulations where all model "j" and "k" values were varied about their associated uncertainties (Crawford et al., 1999).

3. Results and discussion

3.1. OH results

The OH measurements recorded during ANTCI 2003 are shown here as a time series plot in Fig. 1. The individual data entries are presented in the form of 30 s average values. Data gaps in this plot reflect: 1) time periods in which the OH sample inlet was shaded by the ARO building; 2) periods during which there were equipment failure, e.g., during the time period 25 December–29 December; or 3) time periods having data associated with unacceptable instrumental
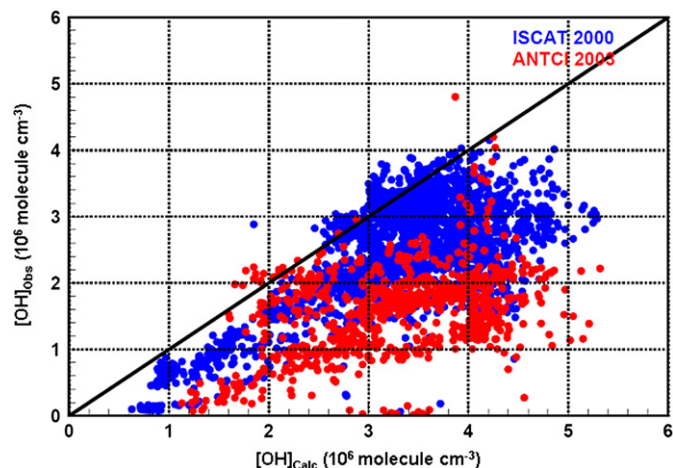

Fig. 2. Plot of observed versus model calculated OH concentrations from the ISCAT 2000 and ANTCI 2003 studies. All model calculations have been constrained by observations of CH_2O and H_2O_2.

parameters such as flows, electrostatic lens settings, electrical noise, or background signal. In a few cases there were also time periods requiring off-line maintenance, diagnostic, or repair work.

As seen in Fig. 1, typical daily average values range from 1.5 to 2.5×10^6 molec cm^{-3}, with occasional values reaching as high as 4×10^6 molec cm^{-3}. These high average values can be largely attributed to the presence of elevated levels of atmospheric NO (Davis et al., 2001, 2004a,b,c). During ANTCI 2003, the median NO value was 231 pptv versus 88 pptv during ISCAT 2000.

In general, the ANTCI 2003 field results have much in common with those generated during ISCAT 2000. This is seen in a more quantitative way in Figs. 2 and 3a. In particular, Fig. 2 reveals that the bulk of the data from both years lies between 1×10^6
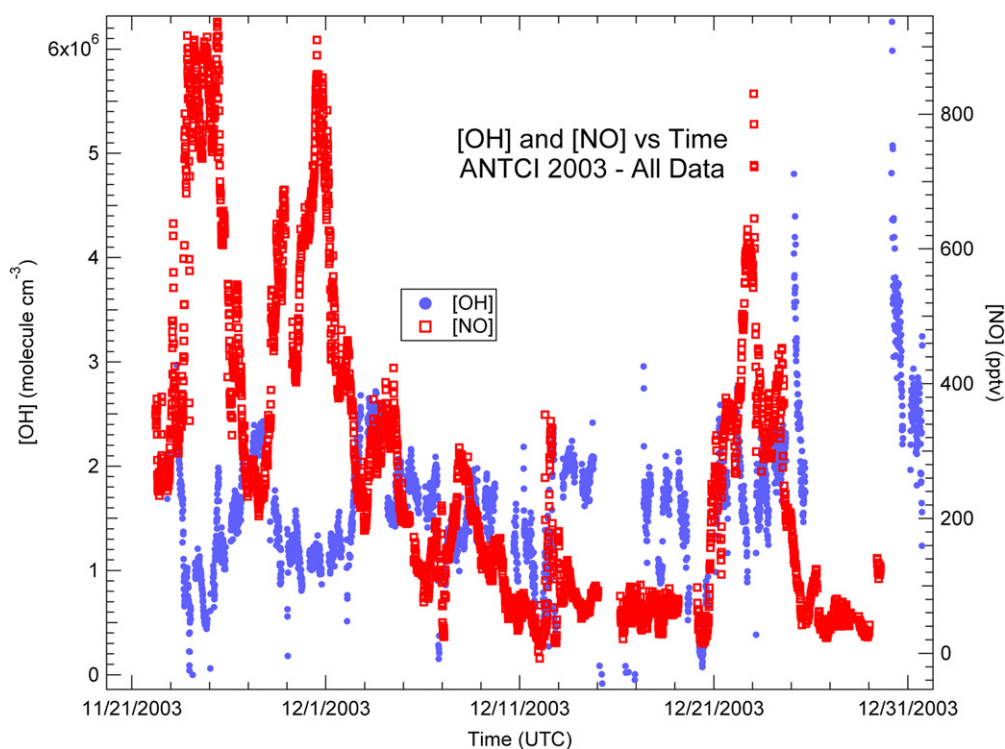

Fig. 1. Plot of measured OH and NO concentrations from the ANTCI 2003 study.
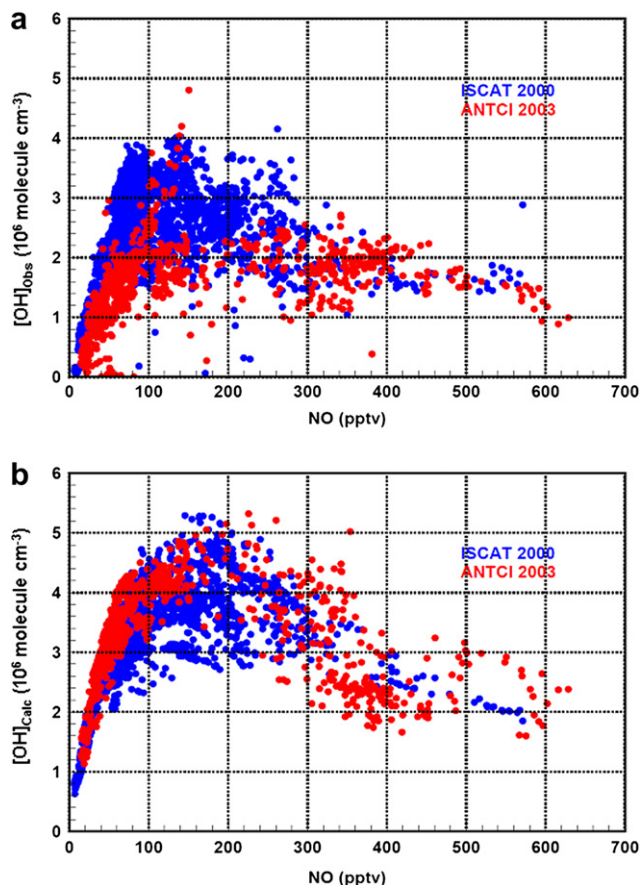
Fig. 3. a. Plot of observed OH concentrations versus NO from ISCAT 2000 and ANTCI 2003 studies. b. Plot of model calculated OH concentrations versus NO from ISCAT 2000 and ANTCI 2003 studies.

molec cm^{-3} and 4×10^6 molec cm^{-3}. Fig. 3a, on the other hand, shows that OH values in both data sets have been strongly influenced by variations in NO with both reaching near maximum values as NO concentrations reach 100–150 pptv. Differences between the two are evident, however, with the 2000 set, on average, being 35–40% higher than those in 2003. It is also rather apparent from Fig. 3a that the most critical NO concentration range leading to the dissimilarity between the two years is that from 100 to 250 pptv. Interestingly, this also is the same concentration range where there is the largest discrepancy between model predictions and observations. At present we have no simple explanation for this perturbation, although it seems unlikely, based on various internal checks of instrument performance parameters, that the cause was instrument related. The fact that there were no extensive observations of the critical species HO$_2$ and HONO during the 2003 study may have been important. One or both of these species may have had a disproportionate influence on the chemistry during the 2003 study.

One aspect of the 2000 and 2003 studies that is quite consistent is that both sets of OH observations are systematically lower than the model predicted values. This may indeed point to the absence of a critical sink reaction in the model mechanism, but potentially of equal importance may be systematic errors in the calibration of the OH instrument. Still a third possibility might involve the presence of systematic losses of OH in the sampling from the ARO site. The latter explanation was earlier discussed in some detail with the most important conclusion being that this problem area could have only resulted in a measured OH value that was too low.

As a way of gaining a somewhat improved understanding of the basis for the difference seen in predicted and observed SP OH levels, we have here examined some of the chemical details of this steady-state photochemical system. In this case the starting point is recognizing that one of the major primary sources of OH at this site is that resulting from the photolysis of O$_3$, (J1).

$$O_3 + h\nu(<330\,nm) \rightarrow O(^1D) + O_2(^1\Delta_g) \tag{J1}$$
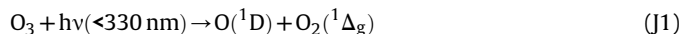
The photolysis product (O^{1}D) rapidly reacts with atmospheric water, (R1) to yield two OH radicals, e.g.,

$$O(^1D) + H_2O \rightarrow 2OH \tag{R1}$$

Quite significant is the fact that the vast majority of the O(^{1}D) is deactivated before it reacts with water due to collisions with the far more abundant atmospheric species N$_2$ and O$_2$. Though not as important as (J1), another primary source of plateau OH is that resulting from the photolysis of H$_2$O$_2$, (J2):

$$H_2O_2 + h\nu \rightarrow 2OH \tag{J2}$$

What makes this a potentially an important OH process at SP is the fact that like NO$_x$, H$_2$O$_2$ is known to be directly released from the snow-pack (Hutterli et al., 2004). Similarly, CH$_2$O can be an important primary source of atmospheric HO$_x$ radicals and also has been shown to have snow emissions (Hutterli et al., 2004). In this case photolysis step, (J3), leads to:

$$CH_2O + h\nu + O_2 \rightarrow CHO + HO_2 \tag{J3}$$

$$CHO + O_2 \rightarrow CO + HO_2 \tag{R2}$$

A final but typically weaker source of HO$_x$ radicals is that resulting from the oxidation of methane, CH$_4$.

In addition to the primary sources of HO$_x$, still another set of reactions that may significantly impact OH levels are the so-called HO$_x$ radical inter-conversion processes. These mainly involve the more abundant HO$_x$ radical species, HO$_2$. At SP the most important of these secondary sources is the reaction of HO$_2$ with NO (R3) with much smaller contributions coming from reaction (R4) involving O$_3$:

$$HO_2 + NO \rightarrow OH + NO_2 \tag{R3}$$

$$HO_2 + O_3 \rightarrow OH + 2O_2 \tag{R4}$$
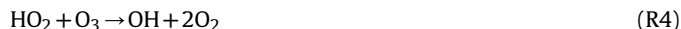
While several of the above processes lead to either the formation or removal of HO$_2$, the single largest source of this radical is the reaction of OH with CO, (R5) followed by (R6):

$$OH + CO \rightarrow CO_2 + H \tag{R5}$$

$$H + O_2 + M \rightarrow HO_2 \tag{R6}$$

Given that the set of reactions cited above forms the core of the steady-state HO$_x$–NO$_x$ photochemical system, it is apparent that for summertime conditions both primary and secondary sources of OH play a critical role in defining the day-to-day variability of this species at SP. In short, this means that the list of controlling species/parameters for OH includes at a minimum: O$_3$, H$_2$O, H$_2$O$_2$, CH$_2$O, NO$_x$, CH$_4$ and UV irradiance. However, due to the dominance of the HO$_2$ species in the plateau atmosphere (HO$_2$:OH, ratio 30:1), plus the fact that primary production from O$_3$ is relatively weak, (R3), supported by elevated levels of NO$_x$, typically dominates as the formation pathway for OH as illustrated in Fig. 3a and b. In both figures, the OH concentration initially increases with increasing NO while values are less than 125–175 pptv. Above this concentration

range, however, it starts to level off; and at still higher concentrations of NO, levels decrease. From model runs, it is can be shown that this initial increase in OH with increasing NO is primarily a consequence of reaction (R3). At still higher NO levels, things become more complex with the results showing that as NO_2 levels increase (e.g., reflecting both increasing rates of (R3) and (R7)), a competing process for OH sets in, (R8), resulting in sufficiently enhanced losses for OH that its trend line becomes flattened.

$$NO + O_3 \rightarrow NO_2 + O_2 \tag{R7}$$

$$NO_2 + OH + M \rightarrow HNO_3 \tag{R8}$$

This "roll over" effect can clearly be seen in Fig. 1 during the large NO enhancement events occurring around 23 and 30 November. In the first case NO concentrations reached nearly 1 ppbv with the corresponding OH concentration dropping to 1×10^6 molec cm^{-3} or lower. Following this early November NO high, NO levels then dropped to ~200 pptv, while OH returned to ~2.5×10^6 molec cm^{-3}. Thus, at this NO concentration, reaction (R1) dominates OH formation while NO_2 levels are still low enough as to not draw-down OH via reaction (R8). Shifting to 7 December, NO levels are seen dropping to even lower values (e.g., ~100 pptv) while OH is also observed dropping to ~1×10^6 molec cm^{-3}. The latter trend can again be understood in terms of the importance of reaction (R3), where with the reduction of NO a substantial reduction occurs in the conversion rate of HO_2 to OH via (R3).

Introducing to the above set of HO_x–NO_x reactions a totally new species such as HONO adds still a new level of complexity to this system. In particular, HONO emissions from the snow-pack not only impact OH, they potentially also can have a significant influence on the NO_x budget. Having a very large photochemical cross section, its lifetime under plateau summertime conditions is only a few minutes. Thus, steady-state levels as low as 10 pptv result in significant shifts in the HO_x–NO_x chemical system, making the need for highly reliable measurements of this species of critical importance. Unfortunately, efforts to measure HONO in Antarctica by our research team as well as others have not resulted in what one might call encouraging results. The most recent attempt by the ANTCI team was during the ANTCI 2003 study (e.g., D. Tan, work in progress). Model runs when constrained by these observations showed minimal correspondence with the OH observational data. Still earlier observations of HONO during ISCAT 2000 actually resulted in predicted OH levels that ranged from factors of two to three times higher than measured at the time. These same HONO observations also have led to problems related to getting closure on the NO_x budget, e.g., see Chen et al. (2004). As a result there still remain major concerns that the HONO measurement techniques now available may yet be suffering from unknown interferences when in an Antarctic setting.

Though not mentioned in our earlier text as a potentially key species influencing HO_x levels, halogens also have frequently been listed as of great importance in polar chemistry studies. This has especially been the case when the site studied has been near the coast (Saiz-Lopez et al., 2007; Jones et al., 2008 and references therein). In several cases direct measurements of one or more gas phase halogen species have confirmed their critical role in the HO_x–NO_x–O_3 chemical system. That they have not been invoked in the current study is a direct result of information gathered by this group in several O_3 studies at SP. The latter have convincingly demonstrated at SP, as well as at other sites on the plateau, that near-surface-chemistry typically leads to the net photochemical generation of O_3 during the Austral spring/summer months (Crawford et al., 2001; Chen et al., 2004; Helmig et al., 2008; Slusher et al., 2002). Since it is well known that halogen species

(particularly bromine and iodine) when present in significant amounts efficiently destroy O_3 (Finlayson-Pitts and Pitts, 2000 and references therein), it follows that the SP O_3 observations are totally incompatible with the idea that halogens play a major role in HO_x chemistry. Even so, some effort to further explore the role of halogen chemistry at plateau sites should be encouraged.

Mechanistically, one of the most significant events that provided a test of current HO_x–NO_x model chemistry was that occurring on 23 November, 2003. The solar eclipse event that took place on this day provided occultation that approached 83%. Thus, in contrast to SP's near constant solar intensity during the summer months, on the 23rd photochemistry was switched "off" very briefly and then back "on". This solar modulation event differed from that caused by clouds in several ways: 1) the change in light levels was uniform unlike those from clouds which tend to be wavelength dependent; 2) the areal effects were also uniform unlike clouds which frequently are localized; 3) the change in light intensity with time was well documented in contrast to clouds where it is typically poorly defined; and 4) whereas, cloud impacts are frequently associated with the passage of a frontal system (leading to both changes in the chemical nature of the air mass as well as in the actinic flux), the chemical changes resulting from the eclipse event involved primarily shifts in the levels of short-lived species. For example, in the latter case the environmental parameters of temperature, pressure, and background chemical composition all remained virtually constant.

As shown in Fig. 4, the eclipse observations reveal major concentration changes in two of the most sensitive photochemical species, OH and NO. (As a point of reference, the degree to which the actinic flux shifted during the eclipse is shown in Fig. 4 in terms of the photochemical rate constant, (J1).) Here, the rapid decrease in NO observed at ~23:15 UT is primarily a reflection of the sudden decrease in its formation rate due to NO_2 photolysis (i.e., (J4)) while still experiencing major losses due to (R3) and (R7).

$$NO_2 + h\nu \rightarrow NO + O \tag{J4}$$

At times greater than 23:15 UT, NO's return to its pre-eclipse level mirrors the return of (J4) to its pre-eclipse value. Like NO, the rapid decline in OH at times approaching 23:15 UT is due to a sudden shift in its formation rate. In this case, it is both the rapid decrease in the primary HO_x formation rate via (J1) and the radical inter-conversion reaction (R3); while still undergoing losses due to reactions (R5), (R8), and (R9):

$$OH + CH_4 \rightarrow H_2O + CH_3 \tag{R9}$$

The return of OH to its more typical value at times >23:15 UT defines the recovery of its formation rate to its pre-eclipse value.

Examining this event in more quantitative terms, it can be seen in Fig. 4 that of the two model predicted profiles generated for OH, when limiting the sources of OH to (J1) (followed by (R2)) and the radical inter-conversion reaction (R3), this "base" model falls quite short of reproducing the magnitude of the OH change. (Note, this model run was implemented since no observations of CH_2O or H_2O_2 were available at that time.) By contrast, inclusion of a new HO_x source based on the assumption of an atmospheric loading of 40 pptv CH_2O due to snow emissions (e.g., reactions (J3) and (R2)), the level of agreement is seen improving considerably. In these simulations CH_2O was used as the new source of HO_x radicals, however, the same effect could have been achieved using snow emissions of H_2O_2:

$$H_2O_2 + h\nu \rightarrow 2OH \tag{J5}$$

In the latter case much higher concentrations would be needed due to the much lower value for (J5). Thus, even mixtures of CH_2O
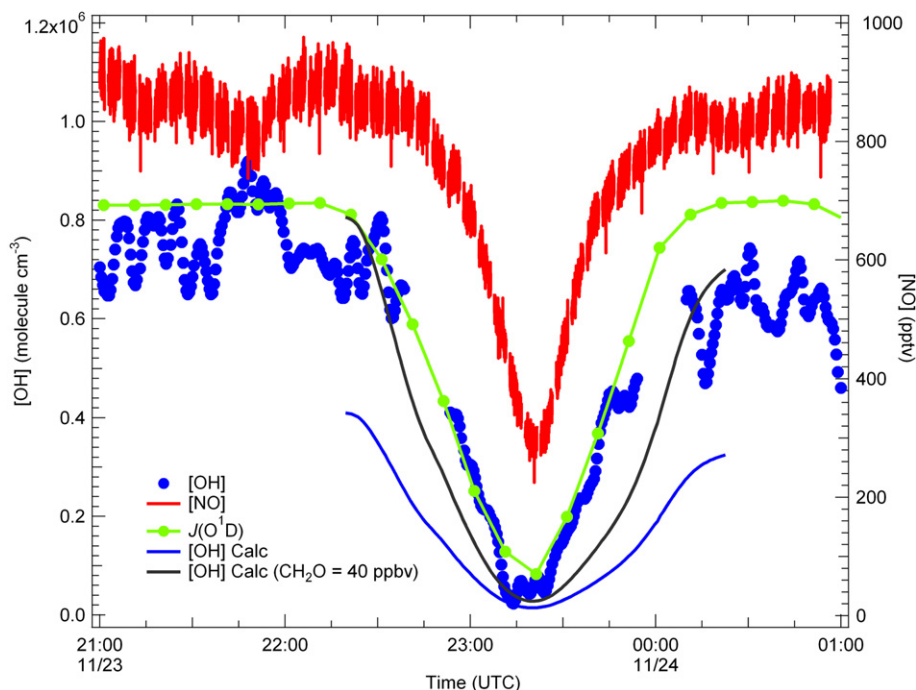
Fig. 4. Plot of observed OH, NO and $J(O^1D)$ values during the 23 November solar eclipse event. OH data are here plotted as a 3-min running average. Values of $J(O^1D)$ are plotted to demonstrate the correspondence between actinic flux fall-off and OH decreases. For reference, the baseline value of $J(O^1D)$ before and after the eclipse is 1.4×10^{-5} s^{-1}. Shown also are model calculated values for OH during the eclipse. Note, for the base run, observations of CH_2O and H_2O_2 were unavailable. A constrained model run is shown assuming a CH_2O abundance of 40 pptv.

and H_2O_2 could have been used. The CH_2O concentration of 40 pptv was selected since it was this level that provided the best match to the observational OH data. However, quite important here is the fact that as already stated the CH_2O constraining the model was assigned to a snow emission source, not a result of CH_4 oxidation. Noteworthy, in the latter regard is that both CH_2O and H_2O_2 were measured two weeks after the eclipse with CH_2O atmospheric levels ranging from 30 to 160 pptv.

Although the final model results shown in Fig. 4, suggest that many of the basic chemical features of the SP near-surface atmosphere appear to be captured by the current model, the match to the observations is still far from being perfect. Even so, the fact that the delta change in OH could be approximated with the addition of CH_2O (or, alternatively, H_2O_2) says much for verifying the importance of snow emissions of these species as primary HO_x sources. The argument here is that the disagreement between model predictions and observations when running the "base" model could not have been greatly influenced by either OH sampling or calibration issues since neither would have a influenced the delta concentration change. Still other missing chemistry in the model could range from the role of HONO, to the role of the more esoteric species HOONO (Nizkorodov and Wennberg, 2002). Even a role for reactive halogens cannot be totally excluded at this time.

3.2. H_2SO_4 results

A time series plot of H_2SO_4 measurements recorded during ANTCI 2003 is shown in Fig. 5. These data include all H_2SO_4 observations made during each of the OH measurement periods as well as those recorded during several solo H_2SO_4 measurement sessions, e.g., building shade time periods. As evident from the plot, the values reported are characteristically low, resulting in a median value of 2.0×10^5 molec cm^{-3} for the time period 21 November–21

December, 2003. Interestingly, this median is quite close to that estimated from the ISCAT 2000 study; and like the earlier study, most of the individual 30 s measurements were near the detection limit. As discussed earlier in Section 2.1, concerns about the evaporation of H_2SO_4 from aerosol surfaces led to our making several "zero" measurements using a denuder assembly. These results indicated that by insulating the inlet and ion reaction region of the SICIMS instrument, the evaporation problem could be greatly minimized. Even so, the measurements reported here still should be considered as an upper limit value for gas phase H_2SO_4.

While the reported H_2SO_4 measurements are, in general, quite low relative to those for OH, a reasonable correlation is still evident between the two species when the focus is on H_2SO_4 peaks. Overall, however, the general trend in H_2SO_4 does not track that exhibited by OH. In particular, the variability in H_2SO_4 is substantially less than that for OH. Since gas phase H_2SO_4 formation involves SO_2 (e.g., (R10–R12)), one might also expect a correlation with this species (e.g., Fig. 5).

$$SO_2 + OH + M \rightarrow HSO_3 \tag{R10}$$

$$HSO_3 + O_2 \rightarrow HO_2 + SO_3 \tag{R11}$$

$$SO_3 + (H_2O)_2 \rightarrow H_2SO_4 + H_2O \tag{R12}$$

Here it can be seen that a qualitative relationship between SO_2 and H_2SO_4 exists for several prominent H_2SO_4 peaks. Of considerable interest is the H_2SO_4 peak emerging on 1 December 2003 and extending forward in time by approximately two days. During this event, SO_2 reaches a peak value of ~40 pptv, then declines to ~7 pptv. At its peak, H_2SO_4 levels range from 0.8 to 1.0×10^6 molec cm^{-3}; but like SO_2, it then drops back to background levels of $2-3 \times 10^5$ molec cm^{-3}. Interestingly, this event also was found to correlate with enhanced aerosol loadings (Arimoto et al., 2008). In
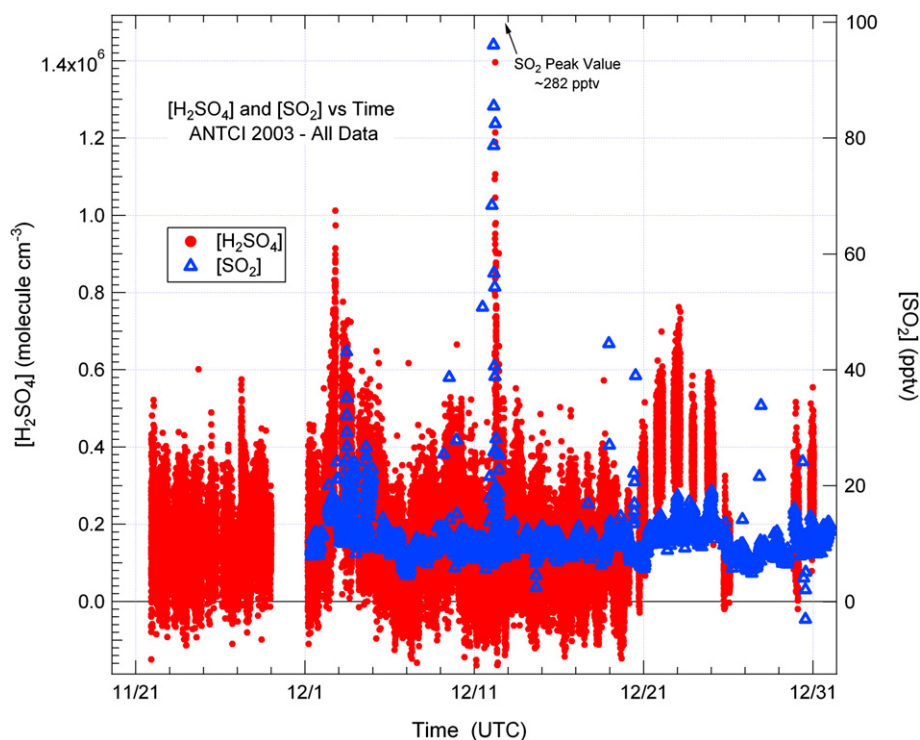
Fig. 5. Plot of observed H_2SO_4 and SO_2 during ANTCI 2003.

this case back air-trajectory analyses revealed that 4–5 days earlier the air parcel sampled at SP had been over the Weddell Sea, a marine region typically rich in DMS emissions. Thus, this event has demonstrated for the first time that non-seasalt sulfate (nss-SO_4^{-2}) levels at SP can be influenced, on occasion, by local chemistry. (Note, in the event cited, a pulse of 40 pptv of SO_2 is capable of generating a nss-SO_4^{-2} pulse of $\sim$120 ng m^{-3}).

Although the above cited case is one involving a natural sulfur source, significant deviations in H_2SO_4 were occasionally attributable to local cases of pollution. The latter can occur when the wind speed at SP drops below $\sim$2 m s^{-1}; and wind direction becomes highly variable, thus permitting SP power station emissions to occasional reach the ARO clean air sector. During one such event on 12 December (e.g., wind speed <1 ms^{-1}) SO_2 reached 282 pptv, yielding a corresponding H_2SO_4 concentration of 1.2×10^6 molec-cm^{-3}. Elevated H_2SO_4 levels are also seen occurring over the time period of 22–24 December 2003. However, the magnitude of the signal in these cases is out of line with locally measured SO_2 levels. This observation in conjunction with the sulfate aerosol data suggests that much of this H_2SO_4 signal is likely due to transport processes involving SO_2 that was oxidized while still much closer to the coast.

The trend in H_2SO_4 as impacted by the solar eclipse event is shown in Fig. 6. Here one sees a rather modest decrease in concentration relative to those for OH and NO. Although no SO_2 measurements were recorded during the eclipse period, there is currently no reason to think that a significant drop occurred during the eclipse. Thus, assuming that the cause for the H_2SO_4 decrease was the draw-down in OH, the lag time displayed by H_2SO_4 suggests an atmospheric lifetime significantly longer than that for OH. Similarly, the much slower rise time for H_2SO_4, compared to OH is indicative of a slower rate of formation than for OH. In this case the rate for reaction sequence (R10–R12) can be compared to that for reactions (J4) and (R3), the latter converting NO and HO_2 to NO_2 and OH.

Using the eclipse observations, the first order loss of H_2SO_4 to pre-existing particles has been defined as simply that equal to the local rate of formation of H_2SO_4, given that the bulk of the H_2SO_4 observed is that produced locally from in-situ SO_2. For this calculation, R10 was taken as 1×10^{-12} cm^3 molec^{-1} s^{-1} for an SP surface temperature of 243 K. Finally, though not measured during the eclipse, the SO_2 concentration was assigned a value of 4.5 pptv based on the best fit generated to the H_2SO_4 eclipse profile. The latter value is approximately a factor of two lower than the average SO_2 concentration measured during the last two weeks of the ANTCI field study, but still well within the day-to-day fluctuations observed in this species. The resulting first order loss rate of H_2SO_4 to particles was estimated at 6×10^{-4} s^{-1}. This value can be compared to the only other available estimate reported of 3.7×10^{-4} s^{-1}, e.g., Mauldin et al. (2004). The latter estimate was based on actual aerosol surface area measurements reported by Park et al. (2004) using data collected during ISCAT 1998 and 2000.

3.3. Methane sulfonic acid results

Fig. 7 shows a time series plot of the MSA data collected during ANTCI 2003. In most cases the observed levels are quite low, typically lying in the range of $1–2 \times 10^5$ molec cm^{-3}. As suggested earlier, a major concern in the measurement of MSA was its relatively high vapor pressure compared to H_2SO_4. However, as was the case for the H_2SO_4 measurements, tests using a denuder assembly revealed MSA concentrations to be $\sim$5–10 times lower than without the denuder assembly. Thus, they suggest it unlikely that evaporation from aerosols had a significant impact on the reported results.

While concentrations are seen as small in Fig. 7, some structure in the time series plot is still evident. Excluding the contamination period, some of this structure appears to be correlated with H_2SO_4. That this would make sense is reflected in the fact that both H_2SO_4 and MSA are final oxidation products from DMS. Interestingly, there
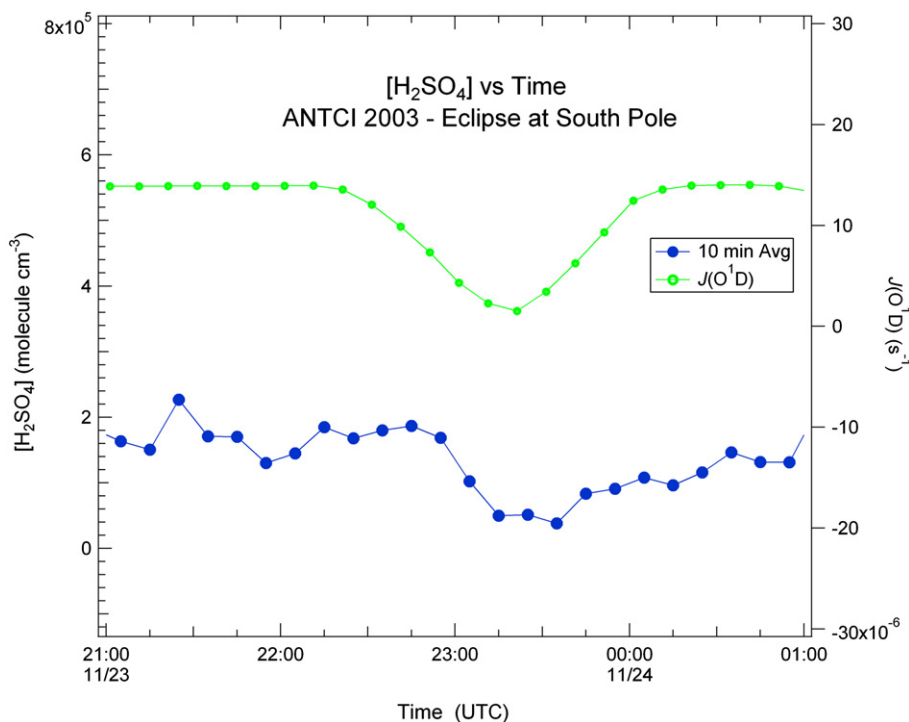
Fig. 6. Plot of observed H_2SO_4 and $J(O^1D)$ as recorded during the 23 November solar eclipse. The H_2SO_4 data are plotted here as 10 min averages.

appears to be no correlative parallel within the DMS observations. This most likely is a reflection of the fact that DMS levels were typically at or near the detection limit for this species, i.e., ~2 pptv.

One of the more interesting aspects of the MSA data is the possible insight they provide as related to the plateau process known as "post-depositional loss". This is a process in which an acidic gas, previously scavenged at the snow's surface, is subsequently focused via snow metamorphosis at the near-surface of the firn and then released back to the atmosphere by evaporation. Glacio-chemists now believe that the species HNO_3, HCl, and MSA are all susceptible to post-depositional loss (De Angelis and Legrand, 1995, Wagnon et al., 1999; Delmas et al., 2003). Regarding
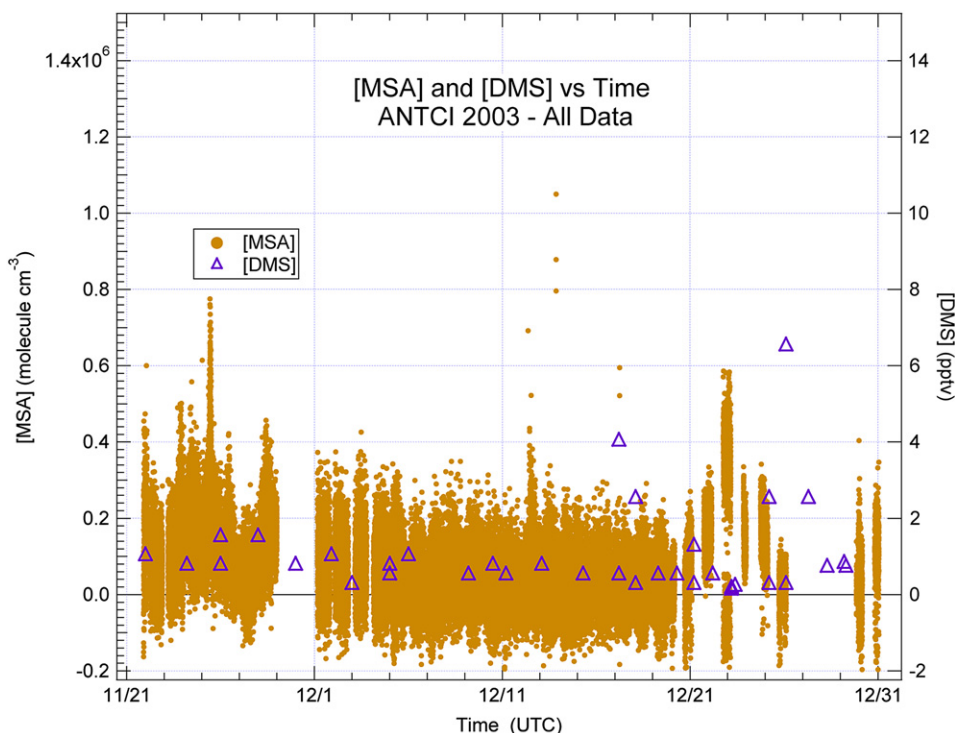

Fig. 7. Plot of observed MSA and DMS as recorded during ANTCI 2003.

MSA, several investigators have suggested that evaporation of this species during the spring/summer season might result in highly elevated levels of this gas on the plateau. However, as seen from Fig. 7 (i.e., median level < 0.01 pptv), the ANTCI 2003 data set does not support this hypothesis, nor do the MSA results from the ISCAT 1998 and 2000 studies. It would thus seem that these collective results point toward there being some highly efficient plateau removal mechanism(s) for MSA. These could be dynamical and/or chemical in nature. One of the simplest of these could involve the physical transport of MSA off the plateau (e.g., via glacial outflow) as reported by Davis et al. (2004c) in the case of NO$_x$. Polar MM5 model runs in conjunction with air back-trajectory analyses by our group suggest that the typical lifetime of an air parcel on the plateau is less than 5 days, with a range of 1–8 days (Arimoto et al., 2008). The second possibility mentioned, chemical processing, most likely would involve the oxidizing agent, OH. Although no kinetic data for this reaction are now available, assuming a modest rate coefficient of 2×10^{-12} cm^3 molec^{-1} s^{-1}, the estimated lifetime for MSA would be only 3 days. Obviously, the fate of MSA on the plateau is one of those areas where further research is needed.

4. Summary and conclusions

The ANTCI 2003 results have confirmed that the SP typically has highly elevated levels of OH during the Austral summer. It has also confirmed that at SP HO$_x$ and NO$_x$ species are tightly chemically coupled with most of the major fluctuations in OH levels being driven by changing concentration levels of NO. The modest but yet systematic difference between the observations and model predictions for both the 2000 and 2003 data bases suggest that there are either missing sinks in the model mechanism and/or difficulties in the measurements due to sampling or calibration issues. The solar eclipse event on 23 November 2003 was of particular significance in that it provided an opportunity to compare model predictions with observations under conditions where the only major factor influencing a species' concentration was the eclipse generated shift in actinic flux. In this context, it was a significant test of the model mechanism in that the observations provided a very reliable delta change in the OH concentration uninhibited by potential problems related to the calibration of the OH sensor or OH sampling issues. Indeed, these results lead one to the conclusion that CH$_2$O and/or H$_2$O$_2$ snow emissions are significant primary sources of HO$_x$ radicals at SP during the Austral summer season. Even so, the deviations seen between the observational and model profiles for OH, even after adding snow emissions of CH$_2$O, suggest that current chemical models may still be missing some critical chemical processes. Speculation here is that species most likely to be involved in these processes are HONO or HOONO with a far lower likelihood that halogen species might be important. Thus far, however, efforts to gain further insight related to the role of HONO have resulted in, at best, mixed results.

For the sulfur species H$_2$SO$_4$ and MSA, the ANTCI 2003 data, like that recorded earlier during ISCAT 2000, have revealed that both are present at very low levels. Typical values were 2×10^5 and 1×10^5 molec cm^{-3}, respectively, although there was some evidence of structure in both profiles. In particular, the H$_2$SO$_4$ profile revealed several interesting peaks where it was evident that levels were sensitive to concentration perturbations in SO$_2$. In a few cases, in fact, the short term enhancements in SO$_2$ were the major driver leading to large enhancements in H$_2$SO$_4$. These SO$_2$ concentration shifts were shown to be due both to natural events (e.g., long range transport) as well as to an occasional local pollution event involving the SP power station.

Although low average H$_2$SO$_4$ concentration levels appear to be consistent with the equally low concentrations observed for DMS, it

has resulted in a mystery as related to MSA. The latter result reflects the current thinking of many glacio-chemists who have suggested that because of its acidic characteristics, post-depositional losses of this species should have generated elevated levels of MSA over much of the plateau. Speculation here is that the answer to this apparent mystery lies in our current lack of knowledge of the efficiency with which MSA is removed from the plateau atmosphere.

As in previous studies carried out at SP, it is apparent that still new investigations using new sampling approaches and new instrumental techniques are much needed. Of particular importance in future studies of HO$_x$–NO$_x$ photochemistry will be the use of an instrument array capable of measuring all critical species simultaneously. Equally important for purposes of addressing both atmospheric and snow photochemical processes will be a need for real-time flux measuring instrumentation. Species high on the latter list are: NO, NO$_2$, HNO$_3$, HO$_2$NO$_2$, H$_2$O$_2$, and CH$_2$O.

References

Arimoto, R., Nottingham, A.S., Webb, J., Schloesslin, C.A., Davis, D., 2001. Non-sea salt sulfate and other aerosol constituents at the South Pole during ISCAT. Geophy. Res. Lett. 28, 3645–3648.

Arimoto, R., Hogan, A., Grube, P., Davis, D., Webb, J., Schloesslin, C., Sage, S., 2004. Major ions and radionuclides in aerosol particles from the south pole during ISCAT-2000. Atmos. Environ. 38, 5473–5484.

Arimoto, R., Zeng, T., Davis, D., Wang, Y., Khaing, H., Nesbit, C., Huey, G., 2008. Concentrations and sources of aerosol ions and trace elements during ANTCI-2003. Atmos. Environ. 42, 2864–2876.

Chen, G., et al., 2001. An investigation of South Pole HO$_x$ chemistry: comparison of model results with ISACT observations. Geophys. Res. Lett. 28, 3633–3636.

Chen, G., et al., 2004. A reassessment of HO$_x$ chemistry based on observations recorded during ISCAT 2000. Atmos. Environ. 38, 5411–5421.

Crawford, J., et al., 1999. HO$_x$ sources over the tropical Pacific based on NASA GTE/PEM data: net effect on HO$_x$ and other photochemical parameters. J. Geophys. Res. 104. doi:10.1029/1999JD900106.

Crawford, J., et al., 2001. Evidence for photochemical production of ozone at the South Pole surface. Geo. Phys. Lett. 28, 3641–3644.

Davis, D., et al., 2001. Unexpected high levels of NO measured at South Pole: observations and chemical consequences. Geophys. Res. Lett. 28, 3625–3628.

Davis, D., et al., 2004a. An overview of ISCAT 2000. Atmos. Environ. 38, 5411–5421.

Davis, D., et al., 2004b. South Pole NO$_x$ chemistry: an assessment of factors controlling variability and absolute levels. Atmos. Environ. 32, 5375–5388.

Davis, D., et al., 2004c. Airborne Observations of NO, NO$_y$, Particles, and Other Trace Gases Over the Antarctic Continent During ANTCI 2003. San Francisco Fall AGU Meeting 2004.

Davis, D., et al., 2008. A reassessment of Antarctic plateau reactive nitrogen based on ANTCI 2003 airborne and ground based measurements. Atmos. Environ. 42, 2831–2842.

De Angelis, M., Legrand, M., 1995. Preliminary investigations of post-depositional effects on HCl, HNO$_3$, and organic acids in polar firn layers. NATO ASI Ser. I30, 362–381.

Delmas, R.J., et al., 2003. Evidence for the loss of snow-deposited MSA to the interstitial gaseous phase in central Antarctic firn. Tellus 55B, 71–79.

Finlayson-Pitts, B.J., Pitts, J.N., 2000. Chemistry of the Upper and Lower Atmosphere. Academic Press, New York, 969 pp.

Helmig, D., et al., 2008. Nitric oxide in the boundary-layer at South Pole during the Antarctic Tropospheric Chemistry Investigation (ANTCI). Atmos. Environ. 42, 2817–2830.

Honrath, R.E., Peterson, M.C., Guo, S., Dibb, J.E., Shepson, P.B., Campbell, B., 1999. Evidence of NO$_x$ production within or upon ice particles in the Greenland snowpack. Geophys. Res. Lett. 26, 695–698.

Honrath, R.E., Peterson, M.C., Dziobak, M.P., Dibb, J.E., Arsenault, M.A., Green, S.A., 2000. Release of NO$_x$ from sunlight-irradiated midland snow. Geophys. Res. Lett. 27, 2237–2240.

Hutterli, M., et al., 2004. Formaldehyde and hydrogen peroxide in air, snow, and interstitial air at South Pole. Atmos. Environ., 5439–5450.

Jones, A.E., Weller, R., Anderson, P.S., Jacobi, H.-W., Wolff, E.W., Schrems, O., Miller, H., 2001. Measurements of NO_x emissions from the Antarctic snowpack. Geophys. Res. Lett. 28, 1499–1502.

Jones, A.E., et al., 2008. Chemistry of the Antarctic boundary layer and the interface with snow: an overview of the CHABLIS campaign. Atmos. Chem. Phys. 8, 3789–3803.

Lurmann, F.W., Lloyd, A.C., Atkinson, R., 1986. A chemical mechanism for use in long-range transport acid deposition computer modeling. J. Geophys. Res. 91, 905–936.

Mauldin III, R.L., Tanner, D.J., Frost, G.J., Chen, G., Prevot, A.S.H., Davis, D.D., Eisele, F.L., 1998. OH measurements during ACE-1: observations and model comparisons. J. Geophys. Res. 103, 16713–16729.

Mauldin III, R.L., Tanner, D.J., Frost, G.J., Chen, G., Prevot, A.S.H., Davis, D.D., Eisele, F.L., 1999. OH measurements during PEM-Tropics A. J. Geophys. Res. 104, 5817–5827.

Mauldin, R.L., et al., 2001a. Measurements of OH, H_2SO_4, and MSA at the South Pole during ISCAT. Geophys. Res. Lett. 28, 3629–3632.

Mauldin, R.L., et al., 2001b. Measurements of OH aboard the NASA P-3 during PEM-Tropics B. J. Geophys. Res. 106, 32,657–32,666.

Mauldin, R.L., et al., 2004. Measurements of OH, $HO_2 + RO_2$, H_2SO_4, and MSA at the South Pole during ISCAT 2000. Atmos. Environ. 38, 5423–5437.

Nizkorodov, S.A., Wennberg, P.O., 2002. First spectroscopic observation of gas-phase HOONO. J. Phys. Chem. A 106, 855–859.

Olson, J.R., et al., 2003. Testing fast photochemical theory during TRACE-P based on measurements of OH, HO_2, and CH_2O. J. Geophys. Res. 109, D15S10. doi:10.1029/2003JD004278.

Park, J., et al., 2004. Aerosol size distributions measured at the South Pole during ISCAT. Atmos. Environ. 38, 5493–5500.

Saiz-Lopez, A., Mahajan, A.S., Salmon, R.A., Bauguitte, S.J.-B., Jones, A.E., Roscoe, H.K., Plane, J.M.C., 2007. Boundary layer halogens in coastal Antarctica. Science 317 (5836), 348–351.

Slusher, D.L., et al., 2002. Measurements of pernitric acid at the South Pole during ISCAT 2000. Geophys. Res. Lett. 29. doi:10 1029/2002GL015703.

Tanner, D.J., Eisele, F.L., 1995. Present OH measurement limits and associated uncertainties. J. Geophys. Res. 100, 2883–2892.

Tanner, D.J., Jefferson, A., Eisele, F.L., 1997. Selected ion chemical ionization mass spectrometric measurement of OH. J. Geophys. Res. 102, 6415–6425.

Wagnon, P., Delmas, R.J., Legrand, M., 1999. Loss of volatile acid species from upper layers at Vostok, Antarctica. J. Geophys. Res. 102, 3423–3431.

Wang, Y., et al., 2008. Assessing the photochemical impact of snow NO_x emissions over Antarctica during ANTCI 2003. Atmos. Environ. 42, 2849–2863.